DOI: 10.31276/VJSTE.65(4).62-70

Chitosan oligomer/silver nanoparticles/PCL composite electrospun membrane for severe burn wound healing

Anh Mai Que[1, 2], Tuan Ngan Tang[1, 2], Tam Phan Thi Thanh[1, 2], Thanh Tu Duong[1, 2], Thanh Binh Vu[1, 2], Van Khiem Nguyen[1, 2], Hoan Ngoc Doan[1, 2], Hiep Thi Nguyen[1, 2*]

[1]*Department of Tissue Engineering and Regenerative Medicine, School of Biomedical Engineering, International University, Vietnam National University - Ho Chi Minh City, Quarter 6, Linh Trung Ward, Thu Duc City, Ho Chi Minh City, Vietnam*
[2]*Vietnam National University - Ho Chi Minh City, Linh Trung Ward, Thu Duc City, Ho Chi Minh City, Vietnam*

Received 2 January 2023; revised 25 February 2023; accepted 28 February 2023

Abstract:

In the management of burn wounds, antimicrobial and wound healing properties are crucial. In this study, we prepared a three-layer electrospun poly(ε-caprolactone) (PCL) membrane for burn wound dressing. The hydrophobic electrospun PCL layer, embedded with silver nanoparticles (SNPs) (PCL-Ag), was coated with another layer of electrospun plasma-treated PCL-Ag to enhance the wettability of the membrane. This enhancement was to facilitate the absorption of the hydrophilic chitosan oligomer (COS) - the third layer of the dressing. The resultant membranes were characterised and tested for different properties to demonstrate their applicability as wound dressing materials. The combination of COS and SNPs of the fabricated membrane supports the healing process and reduces burn severity due to the healing capacity of COS and the antibacterial activity of SNPs, without compromising mechanical strength. We conducted several *in vitro* and *in vivo* experiments to evaluate its applicability for burn wound healing. The PCL-Ag/COS sample demonstrated outstanding *in vitro* biocompatibility and excellent antibacterial activity against *Staphylococcus aureus* strains. We used the membrane to treat burns on rabbits in the laboratory over 30 days, and consistently observed positive outcomes. This research offers insights into the development of bioactive dressings for wound healing and opens up opportunities for practical applications of COS-incorporated materials.

Keywords: **antibacterial wound dressing, electrospun membrane, oligomer chitosan, polycaprolactone, SNPs.**

Classification numbers: **2.2, 3.2**

1. Introduction

Burns are classified as physical, thermal, electrical, radiation, laser, or chemical, depending on the causative agent. Each type of burn wound differs in local and systemic management. Heat not only damages the skin locally but also causes many generalised effects on the body. The increase in capillary permeability caused by heat and damage leads to local reaction (persistent progressive vasodilatation and oedema) as a part of the inflammatory response.

Wound management involves cell proliferation, tissue remodelling, and matrix deposition. Among these, regenerating wound tissue is considered a complex process that involves blood clotting, epithelialisation, wound contraction, and synthesis of collagen and blood vessels. Throughout all these stages, a wound dressing containing antimicrobial agents is required to prevent pathogens from infecting wounds via microbicidal or microbiostatic mechanisms. Dressing materials are typically designed to inhibit bleeding and protect the wound from environmental discomforts. In this context, skin tissues play a critical role in preventing infections caused by microorganisms after trauma. As a result, it is crucial to cover damaged skin with a dressing as soon as possible. Moisture, electrolyte balance, haemostatic, analgesic, healing, and antimicrobial properties must all be maintained. An ideal wound dressing should also be inexpensive, easily accessible, non-allergic, and painless to remove.

Electrospinning (Es) is a versatile, viable, and potentially the most effective and advanced electrohydrodynamic technique [1, 2] for generating continuous ultrathin fibres (down to a few nanometres) from various types of materials, enabling for various applications [2-5]. For tissue engineering and wound dressing, the flexibility to tune the structure, composition, and performance of Es is a great advantage. With a uniform diameter, strong interconnectivity of porosity, high specific surface area, and small pore size, dressings created by this technique can be loaded with bioactive molecules or suitable agents that provide extra functions to meet treatment needs [3, 6-9]. Furthermore, in terms of scale and morphology, these electrospun dressings absorb exudates, inhibit wound drying, and enable gas permeability more efficiency [9].

*Corresponding author: Email: nthiep@hcmiu.edu.vn

In recent years, advances in burn wound care have significantly reduced the incidence of bacterial burn wound infection, altering the epidemiology of infection in burn patients. It has been found that besides bacteria, other micro-organisms such as viruses and fungi are also implicated in burn-related sepsis [10]. A study by Pruitt et al. points out that *S. aureus* and *Pseudomonas* are common pathogens responsible for 48 and 16% of lung infections, respectively. Apart from the increased virulence of organisms invading the wound, there has been no significant change in the statistics of bacterial burn wound infections in the years following B.A. Pruitt, et al.'s study (1992) [10].

The denatured protein in burn-injured tissue provides an ideal environment for microbial growth and proliferation [11, 12]. The ultimate goals of burn management and therapy are to prevent infection, minimise functional impairment, and facilitate wound healing and epithelisation. Wound dressings are created to aid in wound coverage, prevent wound infection, inhibit skin desiccation, and protect against further skin damage. Antimicrobial dressings aim to minimise bacterial colonisation to prevent wound infection. SNPs exhibit broad-spectrum and robust antimicrobial properties against a wide range of microorganisms [13-15]. Despite significant efforts devoted to understanding the origin of the antimicrobial activity of SNPs, the precise mechanism remains elusive [13, 15]. Antimicrobial agents are reported to disrupt the outer membrane of target cells. An important aspect of the antimicrobial activity of SNPs is the synergistic effect that occurs when these particles are combined with other natural and synthetic compounds. Cellular toxicity exhibited by metal nanoparticles slow oxidation through the release of reactive oxygen species and liberate small Ag^+ ions that penetrate through cell membranes, affecting intracellular processes and causing death of the organism [14]. The beneficial effects of silver on wound biology, based on this antimicrobial property, have re-emerged as a viable treatment option for infection-prone wounds such as burns. Some common commercial wound dressings that use ionic silver include Aquacel Ag® (Conva Tec), UrgoClean Ag® (Laboratories URGO), and Silversorb (Medline).

Materials for treating burns and infectious wounds should be biodegradable and environmentally friendly, while also possessing wound healing properties. Chitosan is a polysaccharide macromolecule formed by partial deacetylation of chitin, primarily derived from arthropod exoskeletons and crustaceans. Dressing materials based on chitosan and its derivatives have high durability, good biocompatibility, non-toxicity, and good water uptake capacity [16-19]. Aside from its biocompatibility, biodegradability, and low toxicity, chitosan increases serum protein absorption during wound leaching [16, 20, 21]. Its haemostatic properties, adhesive nature, antifungal and antibacterial effects, and oxygen permeability benefit late-stage wound healing by inhibiting scar formation and promoting epithelial regeneration [16, 22, 23]. However, because of its low molecular weight, COS decreases the overall mechanical strength of the membrane. To compensate for this limitation, polyvinylpyrrolidone (PVP) - a synthetic polymer known for its mechanical stability, swelling behaviour, and low cytotoxicity - is added.

In this study, we present a gamma-assisted one-pot method for preparing SNPs in a non-aqueous mixture of PCL and acetone under varying gamma irradiation doses for the fabrication of electrospun PCL-embedded SNP (PCL-Ag) membranes. An auxiliary solvent, dimethyl sulfoxide (DMSO), was used for the dissolution of silver nitrate in acetone. Prepared solutions were electrospun to form PCL-Ag membranes that undergo plasma treatment (PT) and a coating of COS/PVP solution to create the final antibacterial wound dressing. The obtained membranes were characterised and tested for membrane morphology, mechanical strength, silver release profile, bacterial inhibition, and biocompatibility to demonstrate their suitability as wound dressing materials. The combination of COS and SNPs supports healing in infected wounds and reduces the severity of burns based on the healing capabilities of COS and antibacterial activity of SNPs.

We conducted comprehensive research on the incorporation COS-PCL electrospun membranes and their benefits for wound dressing purpose. The concentrated COS solution created the coating layer with ideal thicknesses and COS densities. To coat the hydrophilic COS onto EsPCL, PT was employed to improve the wettability of the EsPCL membrane. It is expected that this combination possesses synergistic effects between the electrospun PCL and the COS coating layer to improve antibacterial characteristics and biocompatibility of the membranes without compromising mechanical strength. This research provides insights into the development of bioactive dressings for wound healing and paves the way for practical applications of COS-incorporated materials (Fig. 1).

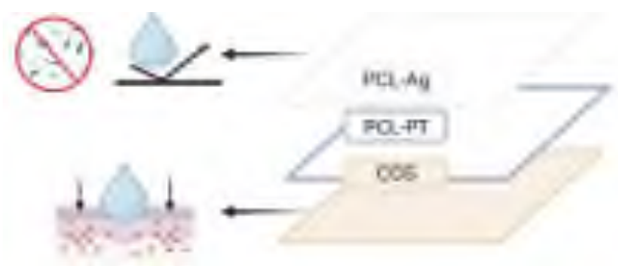

Fig. 1. The ideal design of the PCL-Ag/COS membrane with 3 layers (hydrophobic-adhesive-hydrophilic) using PT.

2. Materials and methods

2.1. Materials

PCL, Mn 80.000, dimethyl sulfoxide (DMSO), acetone (99%), silver nitrate ($AgNO_3$), and MTT (3-(4,5-dimethylthiazol-2-yl)-2,5-diphenyltetrazolium bromide) were purchased from Sigma-Aldrich Co. Ltd., Dorset Gillingham. Mueller Hinton Broth (M391-500G) was purchased from Hi-Media (India). The pathogen, *S. aureus* ATCC 25913, was provided by the Marine Laboratory, International University, Vietnam National University - Ho Chi Minh City. Mouse fibroblast L929 cell line was thawed and cultured in Dulbecco's Modified Eagle Media (DMEM, Gibco, USA) supplemented with 10% foetal bovine serum (Gibco, USA) and 1% penicillin-streptomycin (Gibco, USA).

2.2. Methods

2.2.1. Fabrication of PCL-Ag solution

The SNPs dissolved in PCL solution were synthesised by gamma irradiation following a previously reported procedure [24]. The PCL solution (12 %w/v) was first prepared by dissolving PCL pellets in acetone with stirring at 500 rpm at 60°C for 4 h. After that, a solution of $AgNO_3$ (500 ppm) was added and stirred at room temperature for 10 min. Then, the final solution of PCL-Ag (500 ppm) was obtained by gamma irradiation at 15 kGy. The PCL-Ag (50 ppm) solution was obtained by diluting the PCL-Ag (500 ppm) solution.

2.2.2. Fabrication of membranes: PCL-Ag/PT

EsPCL membranes were fabricated by Es. Parameters were set as following: feed rate of 2.5 ml/h, voltage of 15 kV, rotating speed of 150 rpm/min, a membrane collection area of 60 cm^2, syringe of 10 ml, and 18G needle. The bilayer membranes were electro-spun with three syringes in parallel. The total volume of PCL-Ag solution was 45 ml. The PCL-Ag membrane (10×20 cm) was centred in the plasma chamber (GaLa Instrumented, Germany) to which air plasma was applied for 2 min with 30 W RF power at 13.56 MHz.

2.2.3. Preparation of COS/PVP solution

COS was prepared by diluting the H_2O_2 stock solution (30%) to 6%, then immersing the chitosan powder to obtain 3% (w/v) concentration. The mixture was then magnetically stirred for 24 h at 50°C before microwave irradiation at 400 W (medium) for 2 min to dissolve the residuals. By dissolving PVP powder in the filtered COS solution for 30 min at room temperature, a COS/PVP solution containing 6% (w/v) PVP was obtained.

2.2.4. Coating of COS on the membrane

The EsPCL-Ag/PT membrane was cut into 10x20 cm^2 pieces and sandwiched between two polypropylene frames using double-sided tape and rubber bands to form the mould. A total of 18 ml of COS/PVP solution was evenly spread onto the PCL-Ag/PT membrane 3 times at 6 ml volume each time using a micropipette. Between each coating section, the moulds were placed into a 50°C oven to dry the membrane before more solution was added. The COS-coated sample was denoted as PCL-Ag/COS.

2.2.5. Scanning electron microscope analysis

Membranes were cut into 1×1 cm^2 samples and sputter-coated with Au before microstructures were observed under a scanning electron microscope (SEM, JSM-IT100, Jeol, Japan) at an acceleration voltage of 10 kV. From the SEM images, fibres and pores chosen from random locations were measured using ImageJ software (NIH, USA) to obtain average fibre diameter and pore size. The diameter and pore size data were presented in a histogram to assess the uniformity of the electrospun mats.

2.2.6. SNPs and COS analysis

XRD patterns of the fabricated mats were investigated using D8 Advance Eco, Bruker AXS (Germany) operated at a voltage of 45 kV and a current of 30 mA with Cu Kα radiation (λ=1.54 nm). The 2θ diffraction angles ranging from 30 to 80° (0.2°/step per 0.5 s) were recorded to verify the crystalline structure of the SNPs. Fourier transform-infrared spectra (FT-IR) was employed to observe the interaction between the PCL membrane and chitosan oligomers. The FT-IR spectra were recorded using a Spectrum GX (PerkinElmer Inc., USA) over a wavenumber range of 400-4000 cm^{-1}.

2.2.7. Moisture permeability

The moisture permeability of the electrospun mats was evaluated by moisture vapor transmission rate (MVTR) testing based on BS EN 13726-2:2002 guidelines. Briefly, circular specimens were fixed onto and completely covered by the rims of containers with an area of 10 cm^2. The containers were filled with an appropriate amount of distilled water to ensure that the membranes were 5 mm from the liquid level. Then, the systems were placed in the oven at 37°C for 24 h. The initial (W_1) and final (W_2) weight of water was measured and the MVTR values were calculated using the equation:

$$MVTR = (W_1 - W_2) \times 1000 \ (g/m^2/24\ h) \quad (1)$$

2.2.8. Investigating of controlled release of SNPs

The release testing method (Franz diffusion cells) was used to investigate the *in vitro* release of the SNPs. Release testing was performed in release medium of pH 7.4 (phosphate buffer - PBS) at 37°C. Cellulose acetate membranes (Sartorius®, 0.45 µm average pore size) were used as the artificial

membrane and were maintained in distilled water for 30 min prior to sample membrane loading. At predetermined time intervals (1, 3, 6, 12, and 24 h), a certain volume of sample was withdrawn and replenished with fresh media. Vertical Franz diffusion cells with a volume of 20 ml (contact area: 2 cm^2) were used. After the addition of the release media, cellulose acetate membranes were applied on top of the cell receptor chambers. The donor chambers then were placed on the membranes and tightly clamped. Samples 10 mm in diameter were loaded into the donor chambers and 250 µl of the release media were added to the top of the membrane. The stirring speed of the Franz diffusion cells was set at 600 rpm. At the pre-determined time intervals, 0.15 ml of the media were withdrawn from the receptor chambers and replenished with fresh media. The solution at various times (1, 3, 6, 12, and 24 h) was then taken for ICP-MS analysis to quantify the release of silver content. The experiment was performed in triplicate.

2.2.9. Cytotoxicity

The PCL membrane (control) and PCL-Ag/COS membranes (1×1 cm^2) were soaked in DMEM cell culture (ratio 0.1 g/ml) with 10% bovine serum (Foetal Bovine Serum, FBS) and 1% antibiotic (Penicillin, PS) for 24 h to collect the extract solution. The extract solution was used to culture L929 mouse fibroblasts in a 96-well culture dish at a concentration of 10^4 cells/100 µl/well for 24 h. MTT was added to each well at a concentration of 2 µg/100 µl and incubated for another 4 h. The fluorescence signal was measured at 550 nm. The experiments were triplicated.

2.2.10. In vitro antibacterial experiment

The antibacterial activity of the membranes was evaluated using a strain of Gram-positive bacteria, *S. aureus*, using the antimicrobial fabric zone of inhibition test (AATCC 147). Prior to the experiments, a colony of *S. aureus* strain was extracted from the stock agar plate, placed into a 5-ml Mueller-Hinton broth (MHB) tube, and cultured at 37°C for 24 h. Then bacterial suspension of this strain was prepared by dilution to reach an optical density at 620 nm OD620=0.08-0.1 (equal to 0.5 McFarland standards, approximately 1-2×10^8 CFU/ml).

The microbial susceptibility of each sample against specific bacterial strain was investigated and spread onto a petri dish containing Mueller-Hinton agar (MHA). Briefly, 150 µl of the diluted bacterial suspension was introduced and swabbed evenly on the MHA surface. Then, square membranes of 1×1 cm^2 each were placed on the MHA plate and incubated for 24 h. The bacterial inhibitory zone around the samples was measured.

2.2.11. In vivo animal burn experiment

The *in vivo* wound healing was evaluated by using nine adult male rabbits with an average weight of 2-2.5 kg. Animals were kept at a suitable temperature (27°C) and humidity (40%) for one week before testing. At first, the rabbits were anesthetised by the injection of 50 mg/kg body weight ketamine (10%). For the preparation of the experiment, the hair of the back area of the animals was shaved. The skin area was disinfected with alcohol and the 2nd-degree burn wounds (four full-thickness burn wounds per rabbit) were induced in the surgical area by using a temperature-controlled modified heating instrument. The burn wound (3×3 cm^2 and full thickness) was produced on the back (lumbar dorsal) of each rabbit. The heated template (3 cm diameter) was applied perpendicularly to the designated area with 15 N of pressure and a temperature of 100°C for 15 s [25]. The standard cotton, Betaplast silver, and PCL-Ag/PT/COS dressing were directly applied once a day for 30 d. The animals were randomly divided into three groups with three rabbits in each group. In the control group, the wounds were treated with cotton dressing. The second group was treated with a wound dressing containing PCL-Ag/COS and the third group was treated with the commercial wound dressing Betaplast silver. Animals were caged individually and provided food and water ad libitum. After 30 days, all three groups were euthanised, and the burned tissue was collected.

2.2.12. Burns curing experiment

For 30 days, all three groups of rabbits received dressing changes once per day. The burn wounds were depilated and washed with a solution of povidone-iodine. Each burn wound site was photographed with a camera (Canon, Japan) after 0, 7, 14, 21, and 30 days to measure wound contraction. The photographs were taken directly above the wound. An image analyser (Image J 2.0, NIH, USA) was used to detect wound surface areas during healing. The wound closure percentage (%) was detected as follows:

$$\text{Wound contraction (\%)} = \frac{\text{Wound area at measued day}}{\text{Wound area at the beginning}} \times 100\% \quad (2)$$

2.2.13. Histological examination

The tissue was placed in haematoxylin dye solution for 1 min and rinsed with distilled water. Afterward, the sample was immersed in eosin staining solution for 1 min. Then, dehydration and transparency were performed. Finally, the transparent sample was sealed with neutral gum, observed with an inverted fluorescence microscope, and photographed for analysis.

2.2.14. Statistical analysis

All the data were analysed with statistical software (SPSS 19.0); the measurement data were shown by mean ± standard deviation. By using one-way analysis of variance (ANOVA) with the Turkey post hoc test, with $p<0.05$ indicating the difference is significant and $p<0.01$ indicating the difference is of great significance.

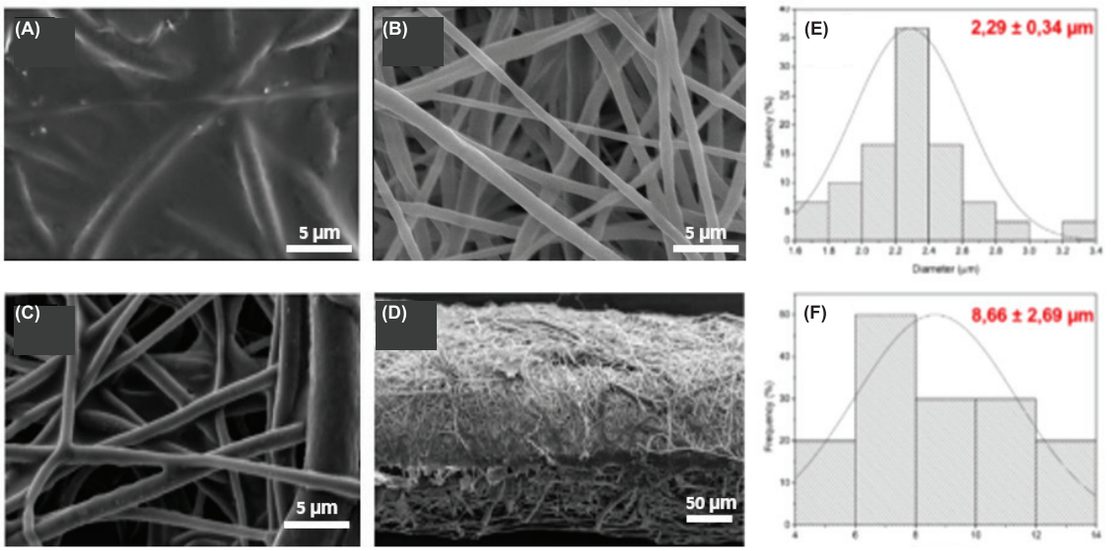

Fig. 2. Morphology of PCL-Ag/COS (A), PCL-Ag (B), PCL-Ag/PT (C), wide view of PCL-Ag/COS (D), distribution of fibre diameter (E), and distribution of pore size (F).

3. Results and discussion

3.1. Membrane characterisation

SEM images of the morphology of the fabricated membrane with different layers are shown in Fig. 2. Under SEM observation, all sample surfaces were macroscopically smooth and microscopically bead-free. The evenly-coated COS on the fibre is shown in Fig. 2A, demonstrated by a thin film of COS covering the fibrous membrane. Three layers of the fabricated membrane are shown in the cross-sectional SEM image (Fig. 2E). Two electrospun outer layers are distinctive while the COS layer, as discussed, is the thin layer at the top. The fabricated PCL-Ag/COS membrane is uniform in fibre diameter (2.29±0.34 µm) with a small pore size (8.66±2.69 µm).

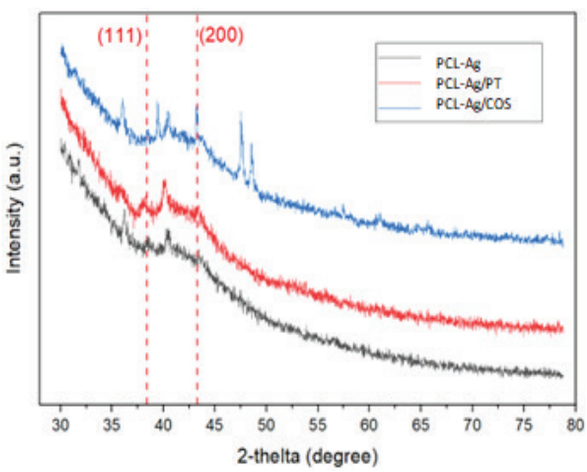

Fig. 3. X-ray diffraction (XRD) patterns of the prepared membranes.

XRD was used to investigate the structure of the SPNs in the membrane (Fig. 3). According to previous studies [26-28], the two peaks at 38.13 and 43.32° correspond to the (111) and (200) planes of the face-centred cubic crystal of silver. The results indicate that the SNPs were successfully incorporated into the PCL membrane.

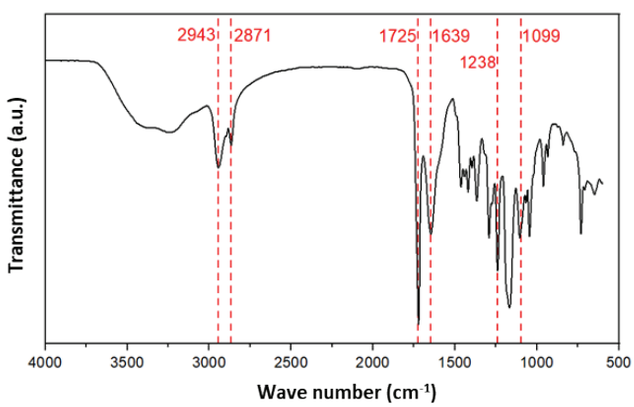

Fig. 4. FT-IR spectra of the PCL-Ag/COS membrane.

FT-IR analysis was carried out to determine the functional groups of COS, as shown in Fig. 4. The broad peak at 3700-3100 cm^{-1} illustrates the stretching motions of the hydroxyl (-OH) and amino (-NH) groups from COS. The vibrations at 2943 and 2871 cm^{-1} are ascribed to the asymmetric and symmetrical CH_2 stretching bands of the material, respectively. Another characteristic peak of PCL is observed at 1725 cm^{-1}, which is from the carbonyl (C=O) groups. Furthermore, the dominant peaks of the base polymer, PVP, are also shown in the FT-IR spectrum at 1639 and 1238 cm^{-1}.

3.2. Controlled release of SNPs

The measurement of SNP release via ICP-MS was also carried out. The result confirmed the presence of SNPs in the membrane (Fig. 5) and also revealed the release behaviour of the silver components from the three membranes. The overall trend of the three samples was the same. Compared to the release profile of PCL-Ag, which was described above, the accumulative concentrations were higher for PCL-Ag/PT and PCL-Ag/COS. In the first 6 h, the Ag concentration of PCL-Ag/PT was 0.72 mg/l while that of PCL-Ag/COS was lower. After 24 h, the release rate of PCL-Ag accelerated, and the concentration reached at 8.40 mg/l. The Ag concentration reached 7.47 and 7.04 mg/l after 24 h for PCL-Ag/PT and PCL-Ag/COS, respectively.

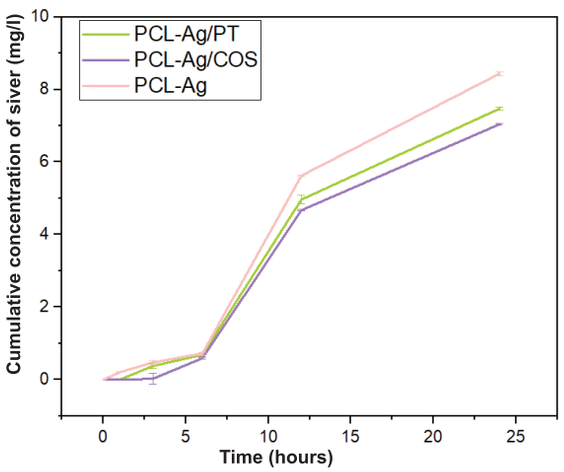

Fig. 5. Quantification of the in vitro release of silver. Cumulative Ag release profiles from the PCL-Ag, PCL-Ag/PT, and PCL-Ag/COS in PBS solution (pH 5.5). Aliquots were taken after 1, 3, 6, 12, and 24 h, then treated with concentrated HNO_3 to convert SNPs into Ag^+ and quantified by ICP-MS (data=mean±SD, n=3).

3.3. Moisture permeability

The moisture permeability is an essential feature of wound dressing, which is to provide sufficient moisture conditions, alleviate the pain, and promote the healing process without dehydration. In numerous studies, MVTR is the standard to evaluate the moisture modulation ability of healing mats [29-31]. The more permeable or breathable the dressing, the higher the MVTR. However, high moisture vapor can lead to wound dehydration, whereas low can lead to wound maceration.

Normal skin has an average MVTR of 204 g/m^2/24 h, while wounds exhibit an MVTR ranging from 279 g/m^2/24 h (first-degree burn) to 5138 g/m^2/24 h (granulating tissue) [32-35]. Although, a suitable MVTR value for moist wound healing was previously defined as 840 g/m^2/24 h [36], recent research has shown that the vapour rate up to 2000-2500 g/m^2/24 h could still provide optimal moisture content for epidermal cells and fibroblasts proliferation [29, 35-38]. As shown in Fig. 6, high MVTRs were observed in all samples, which could be due to the swelling capacities of the fibrous dressings [39]. The cotton dressing had the highest permeability rate (3029±133 g/m^2/24 h), exceeding the recommended value. The thickness of the fabricated membrane impacts its transmission rate, increased layers limit water evaporation through the membrane. When compared to the commercialised product Betaplast silver (1210±56 g/m^2/24 h), our PCL-Ag/COS membrane exhibited a higher MVTR value (1755±84 g/m^2/24 h). Nevertheless, it still maintains a moisture condition conducive to the healing process.

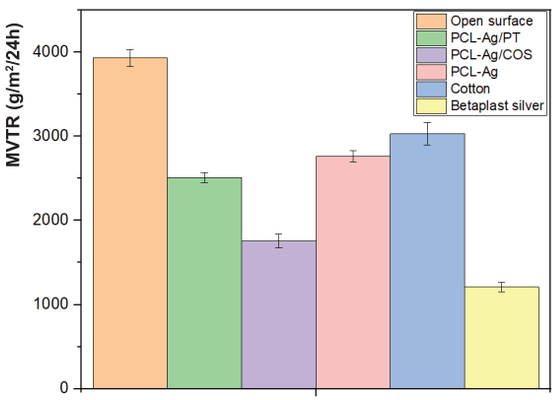

Fig. 6. Moisture vapor transmission rate (g/m^2/24 h) of PCL-Ag/PT, PCL-Ag/COS, PCL-Ag, cotton, and Betaplast silver (data=mean±SD, n=6).

3.4. Cytotoxicity

The MTT assay was conducted to assess cell viability after being cultured in the extract solution for 24 h, providing a measure of the cytotoxicity of the materials. As Fig. 7 illustrates, the 100% extract solution significantly reduced the cell survival rate to a mere 10% compared to the untreated well. This outcome could be attributed to the synergetic effect of the silver and COS from the membranes, aligning with their antimicrobial properties. In fact, a similar reduction in cell viability has also been observed in several commercially available silver dressings such as Aquacel® Ag or Algisite™ Ag [40]. However, it is important to note that when a dressing is applied to a wound, the tissue does not come into contact with the entire extract simultaneously, as in the case with the cultured cells in this *in vitro* test. Therefore, the cytotoxicity level of the 100% extract does not necessarily reflect the actual behaviour of the membrane when applied to tissue. Moreover, cell viability levels in 12.5, 25, and 50% extract solutions were nearly 100% compared to the control, suggesting that the cells can tolerate the membrane components when released kinetically, rather than being exposed to all components simultaneously.

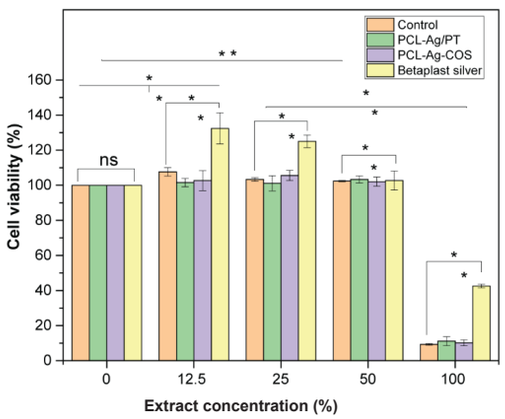

Fig. 7. Viability (%) of fibroblasts after 24 h of incubation in different concentrations of extracted solution of PCL-Ag/PT and PCL-A/COS membranes. Data=mean±SD, n=3, ns: p>0.05, *: p<0.05.

3.5. In vitro antibacterial experiment and related to wound inflammation

The antimicrobial activity of the PCL-Ag/COS membranes was assessed by monitoring their inhibitory zone through agar diffusion tests against Gram-positive strains. Fig. 8 presents images suggesting that SNPs effectively inhibited the growth of the *SA* strain. Regarding *S. aureus*, the PCL-Ag/COS membrane with a low Ag concentration (50 ppm) was sufficient enough to inhibit bacterial growth with a diameter of inhibitory zone of 8.00±0.45 mm.

3.6. In vivo studies

As shown in Figs. 9 and 10, a gradual reduction in wound area can be seen in both the treatment groups (PCL-Ag/COS and Betaplast silver membrane) and the control group (cotton) over a 30-day period. Throughout the observation, no significant difference was observed between the wound sizes of the control and treatment groups. Starting from day 7, the wound area began to change colour and the burn site appeared red, blistered, and potentially swollen. By day 14, the skin of the burn areas had completely receded compared to its original extent. After a month, the wounds in both groups achieved an average wound contraction of 84%. Throughout the 30 days, no signs of infection were seen in the wounds from the treatment and control groups. Minor differences were observed in the extent of granulation and epithelialisation across all wounds. We found the Betaplast silver membrane more difficult to handle during application because of its thickness. Displacement of the dressing from the wound site was more pronounced in the treatment group. Dressings from both groups were only loosely attached to the wounds, causing little pain when they were changed. Compared to the control

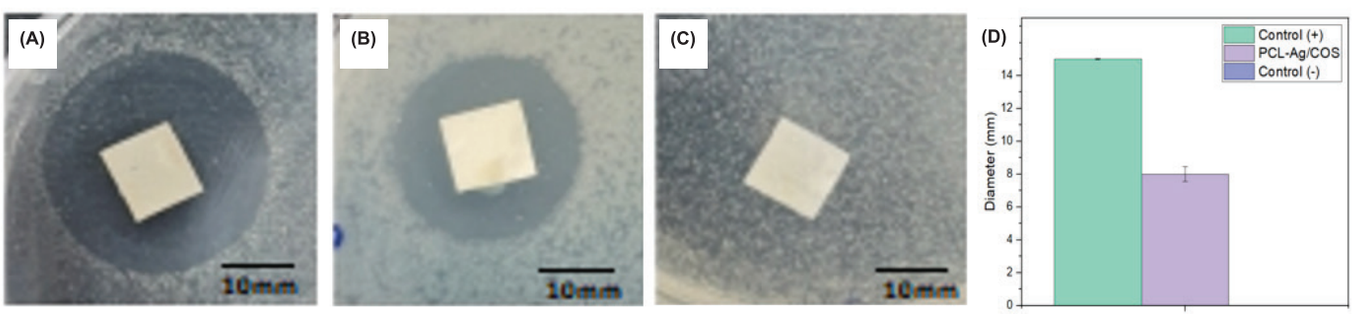

Fig. 8. Images of the inhibition zones formed by ampicillin - positive control (A), PCL-Ag/COS (B), and raw PCL-negative control (C); chart of inhibition diameter of the membranes against *S. aureus* (D).

Fig. 9. Representative images of wounds treated with cotton, Betaplast silver, and the PCL-Ag/COS membranes.

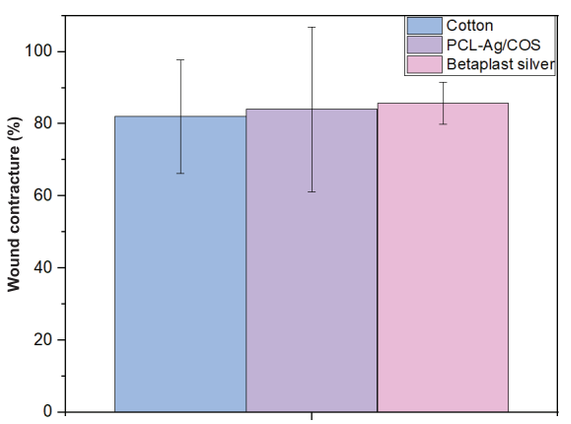

Fig. 10. Wound contracture (%) of wounds treated with cotton, Betaplast silver, and PCL-Ag/COS membranes.

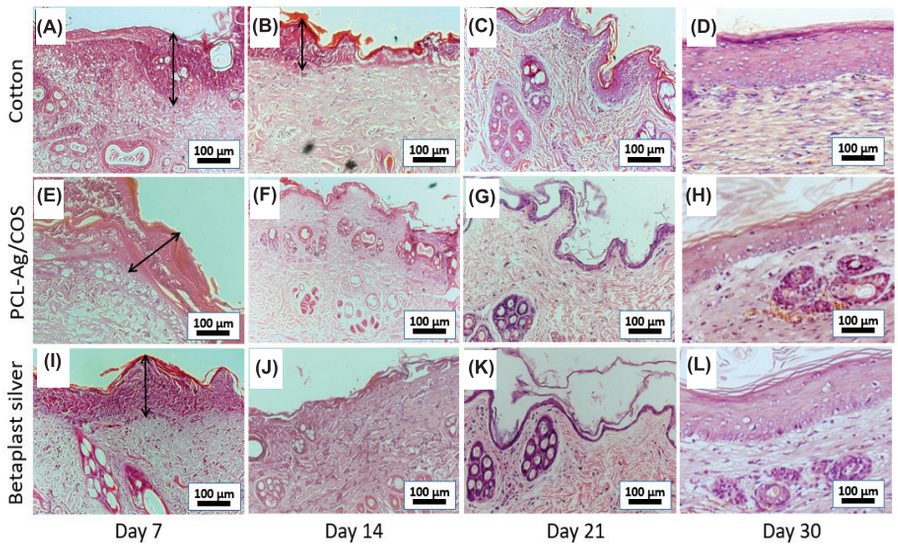

Fig. 11. Histopathology of wound tissue at days 7, 14, 21, and 30 after surgery: wound treated with cotton (A-D), PCL-Ag/COS (E-H), and Betaplast silver membranes (I-L). The arrow indicates the inflammatory area due to the burn wound.

group, dressings from the treatment group were easier to mould to the wound surfaces. Wounds from the treatment group also displayed a larger degree of exudate accumulation beneath the dressings, covering the entire wound surface, while exudate collection from the control group only covered a portion of the wound's surface.

3.7. Histological examination

Histological analyses of the wounds were conducted on days 7, 14, 21, and 30 post-wound creation, as shown in Fig. 11. The H&E straining images successfully demonstrated the creation of secondary degree burn wounds on a rabbit model. By day 7, regenerated granulation tissue had formed in both the dermis and hypodermis, making it difficult to distinguish these layers from normal tissue samples. The thickness of the epidermal layer was inconsistent, and no hair, sweat glands, or fat were observed in the wound area. Wounds dressed with cotton (control) exhibited a thicker inflammatory area compared to those treated PCL-Ag/COS and Betaplast silver dressings, and this inflammation persisted until day 30 of the experiment. The healing process in the treatment groups appeared to progress more quickly, with matrix fibres beginning to synthesise and align in parallel and neatly on day 14 - signals of the granulation phase. In the PCL-Ag/COS group, distinct layers of the epidermis, dermis, and hypodermis could be observed separately, and the thickness of the epidermal layer appeared uniform.

By day 21, tissue re-epithelialisation, fibroblastic proliferation, the formation of a dense collagen mesh, and moderate fibrosis were all observable. By day 30, both treatment groups had transitioned to the inflammation-repair phase more rapidly than the control group. The wounds were covered with healthy epithelial tissue and a new epidermis. The fabricated dressings were found to compatible with the injured tissue, with no evidence of toxicity or irritation that could potentially prolong the inflammatory process.

4. Conclusions

This research outlines the effects of applying a burn wound dressing made of a COS-coated PCL-Ag membrane. The antibacterial properties of both SNPs and COS enhanced the speed of tissue regeneration and healing. Additionally, COS was able to foster optimal conditions for the intricate process of wound healing. In conclusion, the PCL-Ag/COS membrane was successfully fabricated and is suggested as a protective antimicrobial dressing that can aid in the treatment of burn injuries.

CRediT author statement

Anh Mai Que: Conceptualisation, Methodology, Formal analysis, Writing, Editing; Tuan Ngan Tang: Methodology, Editing; Tam Phan Thi Thanh: Conceptualisation, Data analysis; Thanh Tu Duong: Methodology; Thanh Binh Vu: Methodology; Van Khiem Nguyen: Reviewing; Hoan Ngoc Doan: Reviewing, Data analysis; Nguyen Thi Hiep: Conceptualisation, Reviewing.

ACKNOWLEDGEMENTS

This research was funded by the Department of Science and Technology of Ho Chi Minh City under the grant number 01/2020/HD-QPTKHCN.

COMPETING INTERESTS

The authors declare that there is no conflict of interest regarding the publication of this article.

REFERENCES

[1] W.E. Teo, R. Inai, S. Ramakrishna (2011), "Technological advances in electrospinning of nanofibers", *Science and Technology of Advanced Materials*, **12(1)**, DOI: 10.1088/1468-6996/12/1/013002.

[2] J. Xue, T. Wu, Y. Dai, et al. (2019), "Electrospinning and electrospun nanofibers: methods, materials, and applications", *Chemical Reviews*, **119(8)**, pp.5298-5415, DOI: 10.1021/acs.chemrev.8b00593.

[3] B. Ding, X. Wang, J. Yu (2018), "Electrospinning: Nanofabrication and Applications", *Micro & Nano Technologies Series*, **1**, pp.1-88.

[4] J.S. Park (2011), "Electrospinning and its applications", *Adv. Nat. Sci: Nanosci. Nanotechnol.*, **1**, pp.1-6, DOI: 10.1088/2043-6262/1/4/043002.

[5] N. Bhardwaj, S.C. Kundu (2010), "Electrospinning: A fascinating fibre fabrication technique, *Biotechnology Advances*, **28(3)**, pp.325-347, DOI: 10.1016/j.biotechadv.2010.01.004.

[6] Y. Liu, T. Li, Y. Han, et al. (2021), "Recent development of electrospun wound dressing", *Current Opinion in Biomedical Engineering*, **17(1)**, DOI: 10.1016/j.cobme.2020.100247.

[7] M. Rahmati, D.K. Mills, A.M. Urbanska, et al. (2021), "Electrospinning for tissue engineering applications", *Progress in Materials Science*, **117**, DOI: 10.1016/j.pmatsci.2020.100721.

[8] S. Agarwal, A. Greiner, J.H. Wendorff (2013), "Functional materials by electrospinning of polymers", *Progress in Polymer Science*, **38(6)**, pp.963-991, DOI: 10.1016/j.progpolymsci.2013.02.001.

[9] Y. Goh, I. Shakir, R. Hussain (2013), "Electrospun fibres for tissue engineering, drug delivery, and wound dressing", *J. Mater Sci.*, **48(1)**, pp.3027-3054, DOI: 10.1007/s10853-013-7145-8.

[10] B.A. Pruitt, A.T. McManus (1992), "The changing epidemiology of infection in burn patients", *World J. Surg.*, **16**, pp.57-67, DOI: 10.1007/BF02067116.

[11] S. Monstrey, H. Hoeksema, J. Verbelen, et al. (2008), "Assessment of burn depth and burn wound healing potential", *Burns*, **34(6)**, pp.761-769, DOI: 10.1016/j.burns.2008.01.009.

[12] J.L. Macedo, J.B. Santos (2005), "Bacterial and fungal colonization of burn wounds", *Mem. Inst. Oswaldo Cruz*, **100(5)**, pp.535-539, DOI: 10.1590/S0074-02762005000500014.

[13] S. Tang, J. Zheng (2018), "Antibacterial activity of SNPs: Structural effects", *Adv. Healthcare Mater.*, **7(13)**, DOI: 10.1002/adhm.201701503.

[14] A. Ravindran, P. Chandran, S.S. Khan (2013), "Biofunctionalised SNPs: Advances and prospects", *Colloids and Surfaces B: Biointerfaces*, **105(1)**, pp.342-352, DOI: 10.1016/j.colsurfb.2012.07.036.

[15] N. Durán, M. Durán, M.B.D. Jesus, et al. (2016), "SNPs: A new view on mechanistic aspects on antimicrobial activity", *Nanomedicine: Nanotechnology, Biology and Medicine*, **12(3)**, pp.789-799, DOI: 10.1016/j.nano.2015.11.016.

[16] I. Bano, M. Arshad, T. Yasin, et al. (2017), "Chitosan: A potential biopolymer for wound management", *International Journal of Biological Macromolecules*, **102**, pp.380-383, DOI: 10.1016/j.ijbiomac.2017.04.047.

[17] N. Dang, T.T.P. Ho, L.K.K. Nguyen, et al. (2022), "Chitosan oligomer mono-coated and multi-coated nanofibrous polycaprolactone toward the characterization of mechanical strength for wound dressing application", *International Conference on The Development of Biomedical Engineering in Vietnam*, **85(8)**, pp.415-423, DOI: 10.1007/978-3-030-75506-5_34.

[18] T. Ho, V.K. Doan, N.M.P. Tran, et al. (2021), "Fabrication of chitosan oligomer-coated electrospun polycaprolactone membrane for wound dressing application", *Materials Science and Engineering*, **120**, DOI: 10.1016/j.msec.2020.111724

[19] V.K. Doan, K.L. Ly, N.M.P. Tran, et al. (2021), "Characterizations and antibacterial efficacy of chitosan oligomers synthesized by microwave-assisted hydrogen peroxide oxidative depolymerization method for infectious wound applications", *Materials*, **14(16)**, DOI: 10.3390/ma14164475.

[20] T. Dai, M. Tanaka, Y.Y. Huang, et al. (2011), "Chitosan preparations for wounds and burns: antimicrobial and wound-healing effects", *Expert Review of Anti-Infective Therapy*, **9(7)**, pp.857-879, DOI: 10.1586/eri.11.59.

[21] A. Francesko, T. Tzanov (2010), "Chitosan and derivatives for wound healing and tissue engineering", *Biofunctionalization of Polymers and Their Applications*, **125**, pp.1-27, DOI: 10.1007/10_2010_93.

[22] V. Patrulea, V. Ostafe, G. Borchard, et al. (2015), "Chitosan as a starting material for wound healing applications", *European Journal of Pharmaceutics and Biopharmaceutics*, **97B**, pp.417-426, DOI: 10.1016/j.ejpb.2015.08.004.

[23] A. Moeini, P. Pedram, P. Makvandi, et al. (2020), "Wound healing and antimicrobial effect of active secondary metabolites in chitosan-based wound dressings: A review", *Carbohydrate Polymers*, **233**, DOI: 10.1016/j.carbpol.2020.115839.

[24] T.A. Afify, H.H. Saleh, Z.I. Ali (2017), "Structural and morphological study of gamma-irradiation synthesized SNPs", *Polym. Compos.*, **38(12)**, pp.2687-2694, DOI: 10.1002/pc.23866.

[25] A. Oryan, M. Jalili, A. Kamali, et al. (2018), "The concurrent use of probiotic microorganism and collagen hydrogel/scaffold enhances burn wound healing: An *in vivo* evaluation", *Burns*, **44(7)**, pp.1775-1786, DOI: 10.1016/j.burns.2018.05.016.

[26] T. Maneerung, S. Tokura, R. Rujiravanit (2008), "Impregnation of SNPs into bacterial cellulose for antimicrobial wound dressing", *Carbohydrate Polymers*, **72(1)**, pp.43-51, DOI: 10.1016/j.carbpol.2007.07.025.

[27] R. Singh, D. Singh (2014), "Chitin membranes containing SNPs for wound dressing application", *International Wound Journal*, **11(3)**, pp.264-268, DOI: 10.1111/j.1742-481X.2012.01084.x.

[28] M. Oliveira, D. Ugarte, D. Zanchet, et al. (2005), "Influence of synthetic parameters on the size, structure, and stability of dodecanethiol-stabilized SNPs", *Journal of Colloid and Interface Science*, **292(2)**, pp.429-435, DOI: 10.1016/j.jcis.2005.05.068.

[29] M. Butcher (2010), "Moist wound healing, exudate and management of the wound bed", *J. Wound Care*, **19**, Sup.1, pp.10-13, DOI: 10.12968/jowc.2010.19.Sup1.48261.

[30] G. Kannon, A.B. Garrett (1995), "Moist wound healing with occlusive dressings: A clinical review", *Dermatol Surg.*, **21(7)**, pp.583-590, DOI: 10.1111/j.1524-4725.1995.tb00511.x.

[31] K. Vowden, P. Vowden (2017), "Wound dressings: Principles and practice", *Surgery*, **35(9)**, pp.489-494, DOI: 10.1016/j.mpsur.2017.06.005.

[32] P. Zahedi, I. Rezaeian, S.R. Siadat, et al. (2010), "A review on wound dressings with an emphasis on electrospun nanofibrous polymeric bandages", *Polymers for Advanced Technologies*, **21(2)**, pp.77-95, DOI: 10.1002/pat.1625.

[33] C. Chiu, J.S. Lee, C.S. Chu, et al. (2008), "Development of two alginate-based wound dressings", *J. Mater Sci. Mater Med.*, **19(6)**, pp.2503-2513, DOI: 10.1007/s10856-008-3389-2.

[34] L. Liu, X. Li, M. Nagao, et al. (2017), "A pH-indicating colorimetric tough hydrogel patch towards applications in a substrate for smart wound dressings", *Polymers*, **9(1)**, DOI: 10.3390/polym9110558.

[35] R. Xu, A. Niu, J. Li, et al. (2016), "Controlled water vapor transmission rate promotes wound-healing via wound re-epithelialization and contraction enhancement", *Sci. Rep.*, **6**, pp.1-12, DOI: 10.1038/srep24596.

[36] D. Queen, J.D.S. Gaylor, J.H. Evans, et al. (1987), "The preclinical evaluation of the water vapour transmission rate through burn wound dressings", *Biomaterials*, **8(5)**, pp.367-371, DOI: 10.1016/0142-9612(87)90007-X.

[37] J. Powers, C. Higham, K. Broussard, et al. (2016), "Wound healing and treating wounds", *Journal of The American Academy of Dermatology*, **74(4)**, pp.607-625, DOI: 10.1016/j.jaad.2015.08.070.

[38] K.F. Wlaschin, J. Ninkovic, A.J. Young, et al. (2019), "The impact of first-aid dressing design on healing of porcine partial thickness wounds", *Wound Rep. Reg.*, **27(6)**, pp.622-633, DOI: 10.1111/wrr.12747.

[39] J. Boateng, K.H. Matthews, H.N.E. Stevens, et al. (2008), "Wound healing dressings and drug delivery systems: A review", *Journal of Pharmaceutical Sciences*, **97(8)**, pp.2892-2923, DOI: 10.1002/jps.21210.

[40] S. Yunoki, M. Kohta, Y. Ohyabu, et al. (2015), "*In vitro* parallel evaluation of antibacterial activity and cytotoxicity of commercially available silver-containing wound dressings", *Plastic Surgical Nursing*, **35(4)**, pp.203-211, DOI: 10.2147/CWCMR.S72101.